Full Radius Linear and Nonlinear Gyrokinetic Simulations for Tokamaks and Stellarators: Zonal Flows, Applied $E \times B$ Flows, Trapped Electrons and Finite Beta

L. Villard 1), S.J. Allfrey 1), A. Bottino 1), M. Brunetti 1), G.L. Falchetto 5), V. Grandgirard 5), R. Hatzky 2), J. Nührenberg 4), A.G. Peeters 3), O. Sauter 1), S. Sorge 4), J. Vaclavik 1)

1) CRPP - EPFL, Euratom-Suisse, Lausanne, Switzerland
2) Max-Planck Institut für Plasmaphysik, Euratom-IPP, Garching, Germany
3) Rechnungzentrum der Max-Planck Gesellschaft, Garching, Germany
4) Max-Planck Institut für Plasmaphysik, Euratom-IPP, Greifswald, Germany
5) DRFC, Euratom-CEA, Cadarache, France

e-mail contact of main author: laurent.villard@epfl.ch

Abstract. The aim of this paper is to report on recent advances made on global gyrokinetic simulations of Ion Temperature Gradient modes (ITG) and other microinstabilities. The nonlinear development and saturation of ITG modes and the role of $E \times B$ zonal flows are studied with a global nonlinear δf formulation that retains parallel nonlinearity and thus allows for a check of the energy conservation property as a means to verify the quality of the numerical simulation. Due to an optimised loading technique the conservation property is satisfied with an unprecedented quality well into the nonlinear stage. The zonal component of the perturbation evolves to a quasi-steady state with regions of ITG suppression, strongly reduced radial energy flux and steepened effective temperature profile alternating with regions of higher ITG mode amplitudes, larger radial energy flux and flattened effective temperature profile. A semi-Lagrangian approach free of statistical noise is proposed as an alternative to the nonlinear δf formulation. An Asdex-Upgrade experiment with an Internal Transport Barrier (ITB) is analysed with a global gyrokinetic code that includes trapped electron dynamics. The weakly destabilizing effect of trapped electron dynamics on ITG modes in an axisymmetric bumpy configuration modelling W7-X is shown in global linear simulations that retain the full electron dynamics. Finite β effects on microinstabilities are investigated with a linear global spectral electromagnetic gyrokinetic formulation. The radial global structure of electromagnetic modes shows a resonant behaviour with rational q values.

1. Introduction

ITG modes and other microinstabilities are the physics basis of several gyrofluid or gyrokinetic models that attempt to describe anomalous transport in magnetically confined plasmas [1] . The prominent role of zonal flows in the ITG saturation was recognized already some time ago in gyrofluid [2] and gyrokinetic [3] simulations. Through nonlinear coupling of ITG modes a component of the electric field normal to the magnetic surfaces is driven. The $E \times B$ drift of this component, in other words the zonal $E \times B$ flow, in turn reduces the level of ITG turbulence. Thus the zonal component of the perturbation appears as a regulator of the ITG turbulence. It should be ensured that the numerical discretisation scheme does not introduce spurious damping mechanisms in particular of the zonal component, which is linearly totally undamped by collisionless processes [4], since this would affect its amplitude and consequently the ITG turbulence level. At this point the check of energy and particle conservation properties [5] becomes an extremely useful and stringent test of the quality of the numerical simulation.

Methods based on the PIC δf method [6] have been widely used to solve the gyrokinetic equations. Satisfying energy conservation has proven to be technically rather difficult. The main obstacle is to reduce the numerical noise inherent to such methods down to an acceptable level, in other words the challenge is to have a good enough statistics for the gyrocenter tracers. While the parallel nonlinearity was neglected in some works, thus relinquishing underlying energy conservation properties, it was only recently that energy conservation was demonstrated in nonlinear full-radius gyrokinetic simulations, the result of an optimised loading technique that uses the energy conservation as an indicator of the numerical quality [7]-[10]. Results of the application of this method are presented in Section 2 and compared with results without optimisation. The consequences of neglecting the parallel nonlinearity are also shown. A "semi-Lagrangian" formulation is introduced as an alternative to the PIC δf approach.

More physical effects appear when not only the ion, but also the electron dynamics are taken into account. In Section 3 we show the application of a model that assumes adiabatic passing electrons and drift-kinetic trapped electrons to the study of $E \times B$ stabilisation in an Asdex-Upgrade shot with an ITB. Then a model that includes the full electron dynamics is applied to a bumpy cylindrical configuration relevant for W7-X parameters. When finite plasma β is taken into account the microinstabilities become electromagnetic in character. As the toroidal-ITG mode is stabilised with increasing β another mode, called kinetic ballooning mode [11] or Alfvénic-ITG [12], is destabilised with a threshold value below the ideal MHD ballooning limit. We show the results of a global spectral gyrokinetic approach that has allowed us to find a remarkable resonant behaviour of the AITG mode radial structure with rational q values. Finally, the main findings and possible future works are discussed in Section 4.

2. Energy conserving simulations of ITG modes and zonal $E \times B$ flows

In this Section we consider a straight cylindrical configuration. Parameters are pertinent to W7-X: $B_0 = 2.5$T, $a = 0.55$m, $T_i = 5$keV, deuterium, (thus $a = 135\rho_{Li}$), uniform density and T_e profiles, ion temperature gradient with $a/L_T = 3$ peaking at mid-radius. We solve the gyrokinetic equations for ions and a quasi-neutrality equation assuming an adiabatic electron response within cylindrical surfaces. In addition to the $E \times B$ nonlinearity the $v_{||}$ nonlinearity is retained and thus an energy conservation principle is satisfied:

$$\mathcal{E}_{\rm kin} = \int \frac{1}{2} m_i v^2 f d\mathbf{R} d\mathbf{v}, \;\; \mathcal{E}_{\rm field} = \int \frac{q_i}{2} \left(\langle n_i \rangle - n_0 \right) \phi \, d\mathbf{x}, \;\; \frac{\rm d}{{\rm d}t} \left(\mathcal{E}_{\rm kin} + \mathcal{E}_{\rm field} \right) = 0, \qquad (1)$$

where $\langle\rangle$ indicate a gyro-averaged quantity. A finite element, PIC, δf method is used. Pseudo-randomly chosen points in phase space, or "tracers", are evolved according to the gyrocenter trajectories. The quasi-neutrality equation is solved using a finite element method. The right hand side of the quasineutrality equation is calculated by projecting the gyro-average ion density represented by the tracers onto a finite element basis. Statistical noise is inherent to the method. The use of a δf approach [6], in which only the

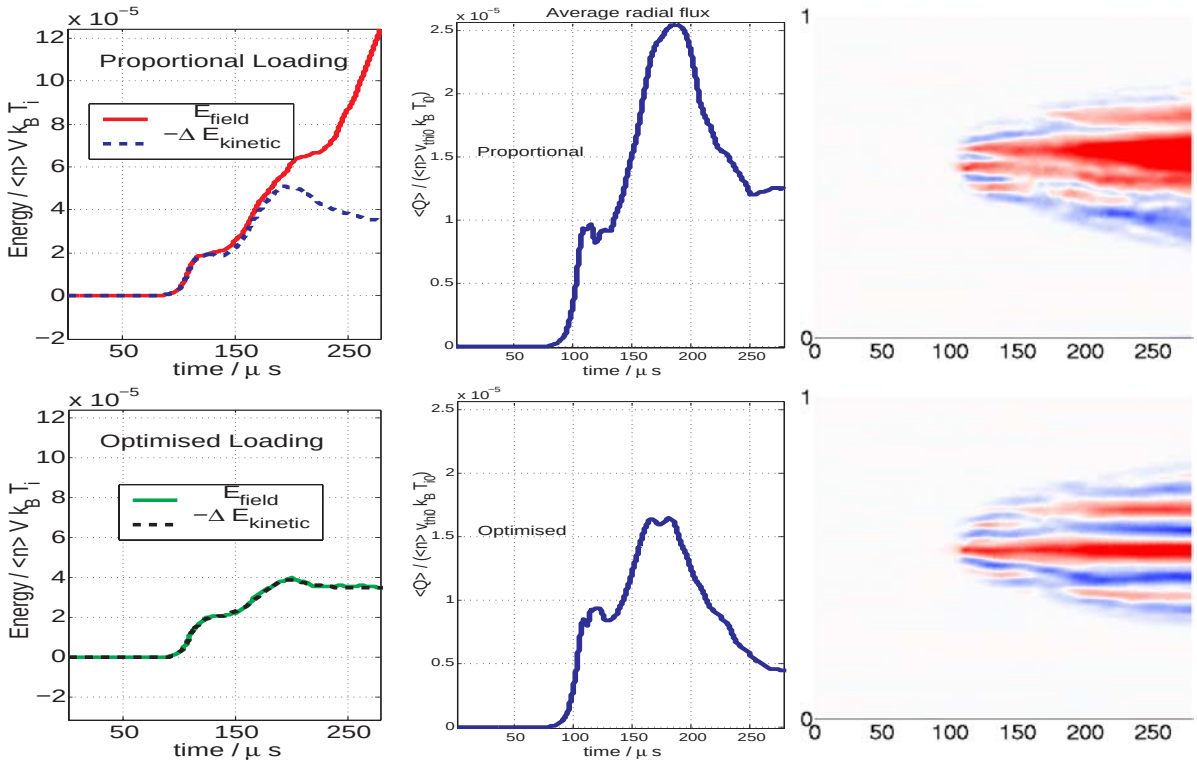

Figure 1: *Field and kinetic energy (left), average radial heat flux (middle) and zonal $E \times B$ component $E_{r00}(r,t)$ versus time, for an unoptimised (proportional) loading (top) and after loading optimisation (bottom).*

perturbed part of the distribution function is used in calculating the right hand side of the quasineutrality equation, greatly reduces numerical noise. By writing $f = f_0 + \delta f$ with f_0 a known background function, the statistical approximation is made not for f but only δf, a function of much lower variance. However, the method can be further improved. The optimised loading technique [7] consists in choosing a distribution of the gyrocenters that minimises this statistical noise. First, a numerical simulation is run with a tracer density proportional to an equilibrium Maxwellian up to a point before the quality of the simulation becomes poor, with the energy conservation serving as an indicator of the quality. The values of $|\delta f|$ are back-mapped to the original tracer positions at time $t = 0$ and a new distribution of tracers is generated from this data. Then a new simulation is performed starting with the new tracer distribution. Eventually, the whole process can be repeated until the desired accuracy is obtained. The bottom line is to increase the density of tracers in active regions of phase space.

We show in Fig.1 the effect of the loading optimisation on the energy conservation, average radial heat flux, and zonal component of the electric field, E_{r00}. It is obvious that the optimisation leads to an excellent energy conservation. A striking feature is that important physical quantities obtained with the proportional loading start to deviate from the physically more correct results as soon as the energy is not conserved ($t > 150\mu s$). In the non-optimised, non-energy conserving simulation the heat flux is a factor of more than 2 too high in the nonlinear stage at the end of the simulation. This large effect on

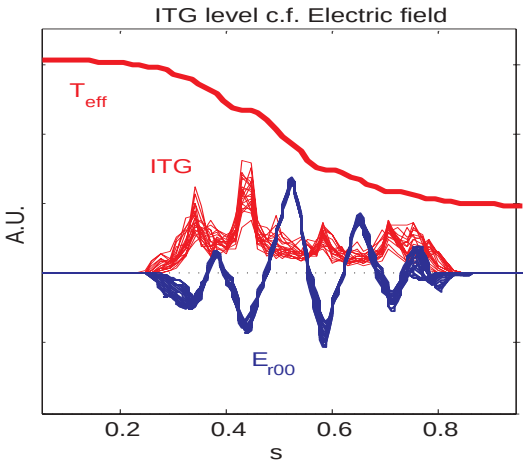

Figure 2: *Snapshots of zonal $E \times B$ flow, ITG amplitude, and effective temperature profiles well into the nonlinear stage of the optimised simulation of Fig.1 around $t = 300\mu$s.*

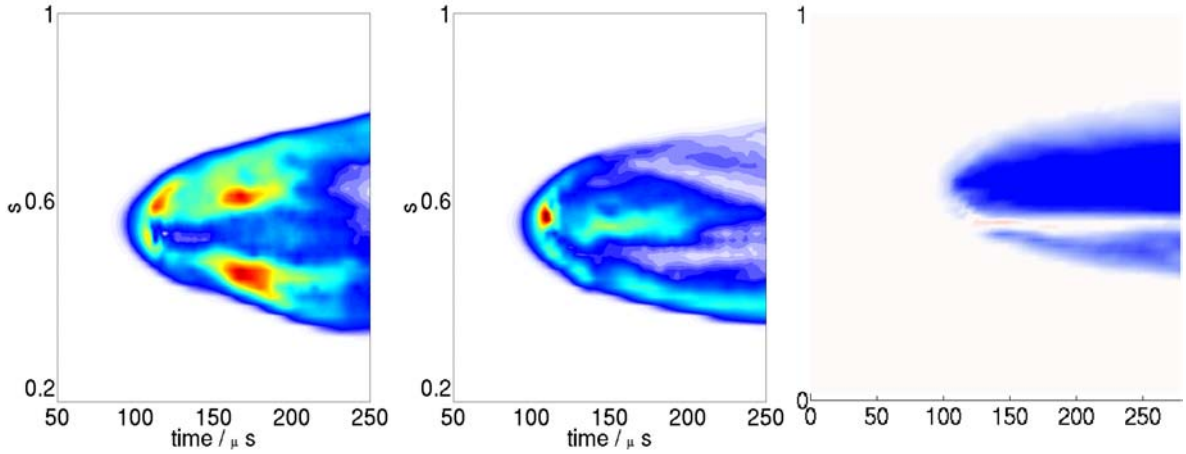

Figure 3: *Radial heat flux vs time and radius with (left) and without (middle) $v_{||}$ nonlinearity. Zonal component of the electric field, E_{r00} vs time and radius without $v_{||}$ nonlinearity (right).*

the predicted heat flux level can be attributed to the incorrect calculation of the zonal component of the electric field: we observe that the regular pattern of E_{r00} as computed with the energy conserving simulation (Fig.1, bottom right), is destroyed at later times in the non-optimised, non-energy conserving simulation (Fig.1, top right). Snapshots around $t = 300\mu s$ of the ITG and zonal component of the electric field (Fig.2) show a remarkable structure with regions of positive E_{r00} coinciding with suppressed ITG mode activity and regions of negative E_{r00} in which ITG modes have a larger amplitude. The effective ion temperature profile is steepened in the suppressed ITG regions and flattened in the active ITG regions.

We have confirmed the pivotal role of the zonal component of the electric field in artificially suppressing it: we have found a radial heat flux an order of magnitude higher. This seems to imply that the strongest nonlinearity in the system is the $E \times B$ nonlinearity. However, one should not conclude that the $v_{||}$ nonlinearity is negligible. The main consequences of ignoring it are the absence of parallel ion trapping, therefore affecting nonlinear ion Landau damping, but also that the energy conservation property is not satisfied and therefore a precious indicator of the quality of the numerics is lost. We per-

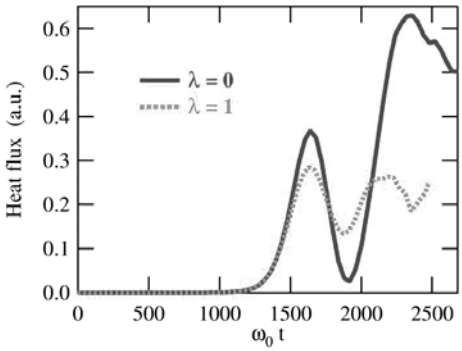

Figure 4: *Heat flux without (full line) and with (dashed line) zonal flows, obtained in a semi-Lagrangian nonlinear drift-kinetic simulation.*

formed a simulation with the same physical and numerical parameters as the optimised loading simulation of Fig.1 but cancelling the term $(q_i/m_i)\langle \mathbf{E} \rangle \cdot \mathbf{e}_{||}$ in the equation for $dv_{||}/dt$. The results were strongly affected by this modification. A Fourier decomposition of the field energy shows in particular that all components with $m = 0, n \neq 0$ are entirely unpopulated. The zonal $E_{r00}(r,t)$ pattern is strongly affected and with it the radial heat flux (Fig.3). (Note that a similar important role of the parallel velocity nonlinearity, but on electrons, was found in the case of drift wave turbulence [13]).

An alternative to the PIC-δf method is the semi-Lagrangian approach. This method retains both an Eulerian aspect in that the phase space is discretised on a fixed grid and a Lagrangian aspect in that the gyrocentre trajectories are computed (characteristics) to obtain the evolution of the full distribution function f. The integration along characteristics is performed with a time-splitting algorithm which allows one to divide the resolution of the advection equation as a succession of 2D and 1D advections. Cubic spline interpolations are performed to evaluate the value of f at the feet of the characteristics. Preliminary results [14, 15] of a new code written for the cylindrical geometry and assuming drift-kinetic ions and adiabatic electrons show that the linear properties are well reproduced, that the zonal flows indeed have a prominent role in the saturation mechanism (see Fig.4), and that the energy conservation property can be satisfied with reasonable accuracy. The parameters used in these computations were for a small cylinder plasma of radius $10\rho_{Li}$, constant density and T_e profiles, a T_i profile with maximum gradient at mid radius and $a/L_T = 4$. The reason to choose these parameters were to investigate the numerical properties of the semi-Lagrangian approach and to have a quick benchmark versus PIC methods. Our results so far indicate that all features of the linear stage of the simulation are in very good agreement with PIC codes (growth rates and mode structures). The behaviour of the nonlinear stage is qualitatively similar to that given by PIC codes, but there remains a discrepancy to be resolved in the level of saturated mode amplitudes.

3. Effects of non-adiabatic electron dynamics and magnetic curvature

The non-uniformity of the magnetic field along the field line creates trapped particle populations and can affect microinstabilities in various ways. For example, trapped electrons tend to respond non-adiabatically and their presence is overall destabilising. In

previous works it was shown that equilibrium radial electric fields and their associated $E \times B$ flows in tokamak and heliac configurations stabilize toroidal, helical and slab ITG modes with a quadratic dependence on the shearing rate, whereas trapped particle modes can be *destabilized* by $E \times B$ flows [8, 16, 17]. We consider Asdex-Upgrade shot no.13149

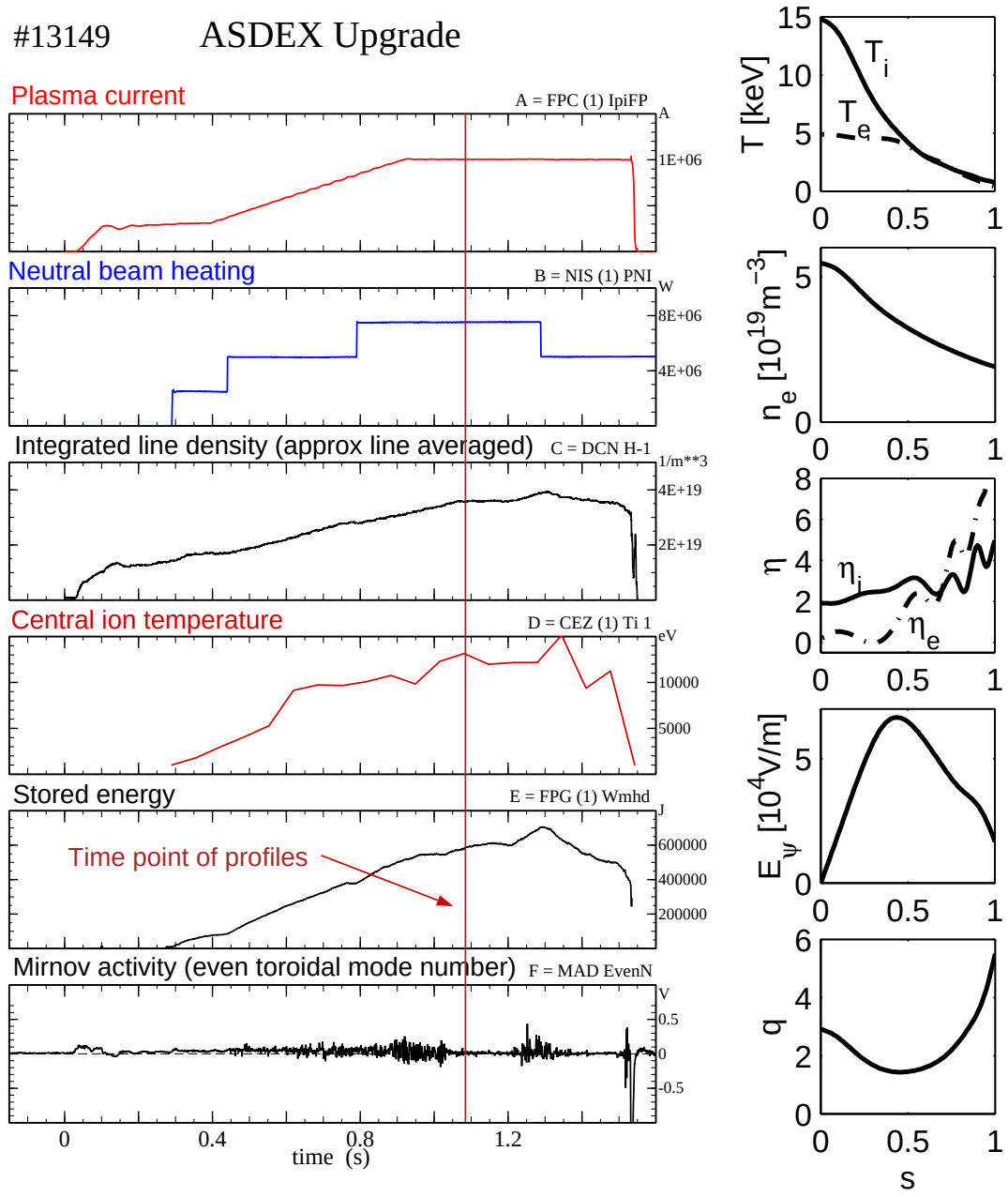

Figure 5: *Time traces and equilibrium profiles of Asdex-Upgrade shot no.13149.*

in which an Internal Transport Barrier (ITB) for ions was formed (Fig.5). We study the global linear stability properties with a model that includes the non-adiabatic trapped electron response and the equilibrium radial electric fields [18]. Considering the actual (reconstructed) ideal MHD equilibrium configuration and profiles of electron temperature and density, but setting a uniform ion temperature and ignoring the radial electric field E_ψ, the most unstable mode found is a trapped electron mode (Fig.6, left). Considering

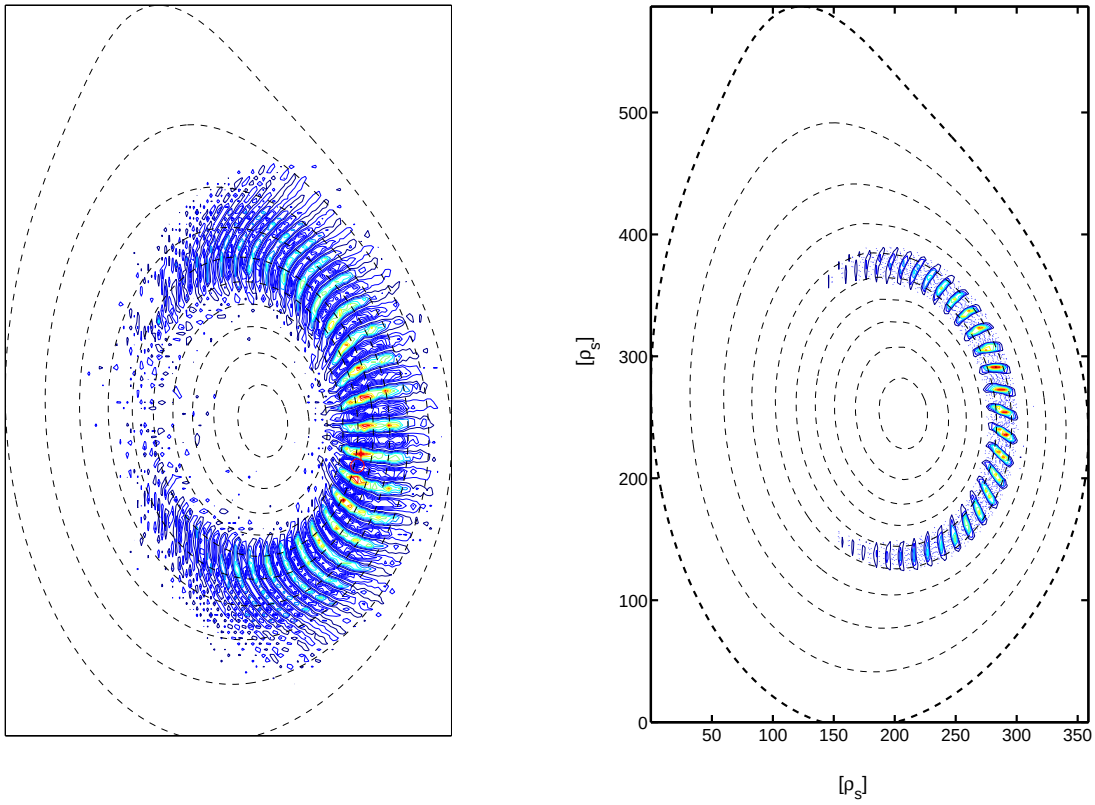

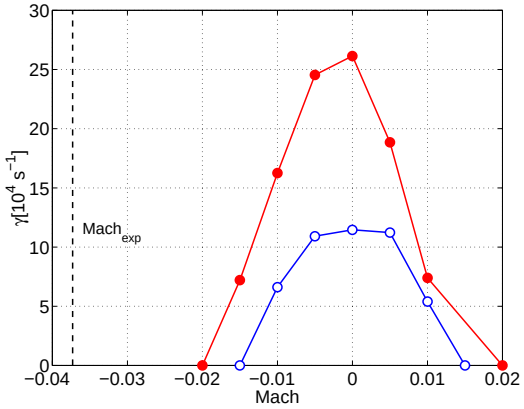

Figure 6: *Top left: Trapped Electron Mode calculated for Asdex-Upgrade shot no.13149 assuming experimental equilibrium profiles except a flat T_i and no radial electric field. Top right: ITG mode calculated for Asdex-Upgrade shot no.13149 assuming experimental profiles (including T_i) but no radial electric field. Right: growth rates of the most unstable mode vs equilibrium $E\times B$ velocity assuming adiabatic electrons (open circles) or drift-kinetic trapped electrons (filled circles). Dashed line: experimental Mach value.*

also the actual T_i profile but still ignoring the radial electric field, we show in Fig.6 (right) the most unstable mode found: it is a toroidal-ITG mode further destabilised by trapped electrons that is localised near the foot of the ion ITB. We then consider the equilibrium radial electric field and study the linear growth rate as a function of the Mach number of the $E \times B$ velocity, by scaling the experimental profile by a series of constant factors. Fig.6 (right) shows that for the value inferred from experimental measurements (dashed line) the modes are completely stabilised. We have performed the computations using the assumption of a fully adiabatic electron response and repeated the calculations with adiabatic passing electrons but non-adiabatic (drift-kinetic) trapped electrons. in both cases full stabilisation is reached when the equilibrium electric field is taken into account. In that experiment the inferred ion heat diffusivity was improved not only at the ITB location but in the whole volume interior to it, a region of negative shear. In

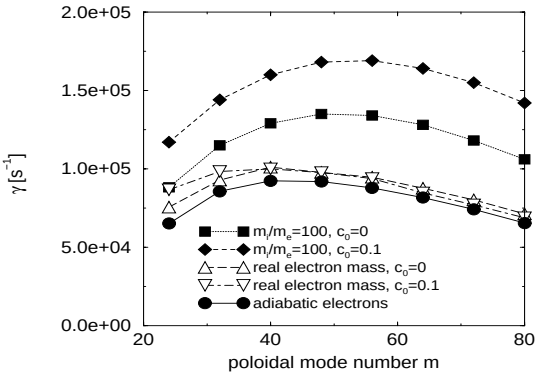

Figure 7: *Growth rates of $n = 2$ modes vs m calculated for different bumpiness parameters c_0 and ion to electron mass ratios, in a global simulation with both gyrokinetic ions and electrons, for W7-X-like parameters.*

order to understand this, we have performed numerical simulations with all parameters as for the experiment, save for considering a temperature gradient localised around some region. Our results show that the ITG modes (including trapped electrons) are stable throughout the reversed shear region, but unstable outside. The presence of the ITB in this shot is therefore compatible with $E \times B$ stabilisation of ITG modes, even when the destabilising non-adiabatic trapped electron response is considered. We have started the analysis of another Asdex-Upgrade shot in which no ITB was formed. First results indicate that even when taking into account the equilibrium electric field an unstable Trapped Electron Mode subsists.

We now consider an axisymmetric bumpy equilibrium configuration in which the dominant non uniformity of B is a mirror term.

$$\vec{B}(r,z) = B_0[\vec{e}_r N c_0/(2R_0) r sin(Nz/R_0) + \vec{e}_z(1 + c_0 cos(Nz/R_0)], \qquad (2)$$

where N is the periodicity of the system (in this case N=5). For $c_0 = 0.1$, one gets 28% trapped particles for a major radius $R_0 = 5.5m$, a minor radius $a = 0.55m$ and a field strength $B_0 = 2.5T$. These are typical parameters for the W7-X stellarator. Both ions and electrons are modelled as fully gyrokinetic. Fast electron motion introduces constraints on the time step and can increase numerical noise. The difficulty is overcome by using the optimised loading scheme which allows us to reach numerically converged results with a substantially reduced number of gyrocentre tracers. The influence of the trapped particles and electron inertia is shown in Fig.7. Considering an artificial $m_i/m_e = 100$ mass ratio we observe that including the magnetic field bumpiness is overall destabilising (diamonds and squares in Fig.7). However, as the mass ratio is increased this destabilising effect decreases and for the physical mass ratio becomes practically negligible (open triangles in Fig.7). We note also that electron inertia is destabilising even in the straight cylinder configuration. Finally, with a field bumpiness comparable to that of W7-X and for a real electron mass, we note that the ITG growth rates are very close to the adiabatic electron model prediction (circles in Fig.7).

We have extended the global spectral approach of Ref.[19] to electromagnetic perturbations with a two-potential formulation $(\phi, A_\parallel)$, (thus neglecting the perturbed parallel magnetic field). All orders in ion Larmor radius are retained and non adiabatic drift-

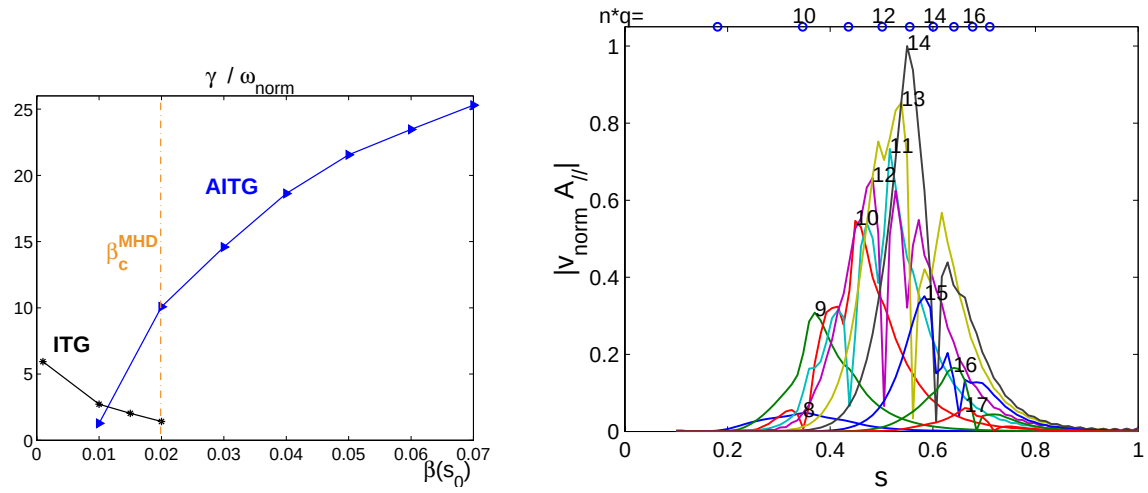

Figure 8: *Left: growth rate of ITG and Alfvénic-ITG (AITG) modes vs beta, critical β for ideal MHD ballooning (vertical line), normalised to* $\omega_{\rm norm} = 3 \cdot 10^4 {\rm s}^{-1}$. *Right: radial structure of AITG eigenmode showing resonant behaviour at rational q values indicated by the circles on top axis.*

kinetic electrons are included in the model. The formulation is applied to a large aspect ratio toroidal configuration [20]. Our results (Fig.8, left) show that as β is increased, the toroidal-ITG growth rate decreases. At a β value about half the critical β limit for ideal MHD ballooning modes, another mode (AITG) is destabilised, qualitatively confirming earlier results [11, 12, 21]. The remarkable feature obtained with our global approach is the eigenmode structure. Fig.8 (right) shows the radial structure of the modulus of poloidal Fourier components of $A_{||}$. At rational q surfaces (circles on top axis) the corresponding m amplitude goes to zero with a sharp localised radial gradient. This behaviour is due to the non-adiabatic electron response: the ratio $|\omega|/k_{||}v_{the}$ varies from much smaller than unity far from the rational surfaces to larger than unity in their vicinity. We note that such a mode structure cannot be found with electron fluid models. It is of course unaccessible to local models that assume e.g. $k_{||} \approx 1/qR$ or to models based on first order ballooning approximation. The sharp radial structure implies that $k_\perp \rho_{Li} \sim 1$, and thus models that use low order expansions in $k_\perp \rho_{Li}$ may be inaccurate. Our approach overcomes all these difficulties.

4. Discussion and future directions of work

We have demonstrated the pertinence of using the energy conservation principle as an indicator of the quality of nonlinear global gyrokinetic simulations. The optimised loading technique is very effective in improving this quality. We have observed a clear correlation between the achieved accuracy of the energy conservation and that of other important physical quantities such as the heat flux or the zonal component of the perturbation. The importance of retaining the $v_{||}$ nonlinearity has also been evidenced. The pivotal role of the zonal component of the perturbation has been confirmed. We have shown

how the system establishes a particular radial structure with regions of reduced heat flux alternating with regions of higher heat flux. The zonal component of the electric field, once this structure is established, stays quasi-steady on much longer time scales as compared to the inverse linear growth rates of ITG modes. The question arises as to how to use the global gyrokinetic results for transport modelling. A local diffusion coefficient can obviously not reproduce the observed nonlocal, structured features of heat flux. The optimised loading scheme has very recently been implemented in the toroidal version of the code and first results indicate that it does also improve the quality of the simulations [22].

We have shown the consistency of the presence of an ITB in an Asdex-Upgrade experiment with the $E \times B$ stabilisation, even when the usually destabilising non-adiabatic trapped electron response was taken into account. First results on another Asdex-Upgrade discharge in which no ITB was formed indicate that a trapped electron mode is still unstable even when the experimental profile of equilibrium radial electric field is considered. A more detailed analysis will be performed in the future.

We have shown that trapped electron dynamics is only weakly destabilising ITG modes in a bumpy configuration modelling W7-X. Global gyrokinetic computations using the full 3D geometry of the equilibrium magnetic field [23] show that ITG modes are rather weakly coupled by 3D geometrical effects in W7-X [24] and growth rates are close to those obtained in a straight cylinder. This gives some justification for the relevance of the simplest geometry (cylinder) and the simplest electron model (adiabatic) used in our nonlinear simulations. Of course more work is needed to ascertain this hypothesis.

We have shown that the inclusion of electron dynamics and electromagnetic effects creates a resonant radial structure of the unstable modes at rational q values. Further works, in particular nonlinear global electromagnetic gyrokinetic simulations, may well be needed before concluding this could be related to the resonant behaviour of electron transport observed in some tokamaks. Even though it should be recalled that all the works presented in this paper were calculated without collisional effects, it is interesting to note that the resonant behaviour at rational q surfaces of the electromagnetic modes we found resembles that of tearing modes.

Acknowledgements. Fruitful discussions with Drs. T.S. Hahm and Y. Idomura are gratefully acknowledged. This work was partly supported by the Swiss National Science Foundation.

References

[1] DIMITS A.M., BATEMAN G., BEER M.A., et al., Phys. Plasmas **7** (2000) 969.

[2] HAMMETT G.W., BEER M.A., DORLAND W., COWLEY S.C., SMITH S.A., Plasma Phys. Controlled Fusion **35** (1993) 973.
[3] SYDORA R.D., DECYCK V.K., DAWSON J.M., Plasma Phys. Controlled Fusion **38**, (1996) A281.
[4] ROSENBLUTH M.N., HINTON F.L., Phys. Rev. Lett. **80** (1998) 724.
[5] HAHM T.S., Phys. Plasmas **3**, (1996) 4658.
[6] DIMITS A.M., LEE W.W., J. Comput. Phys. **107** (1993) 309.
[7] HATZKY R., TRAN T.M., KÖNIES A., KLEIBER R., ALLFREY S.J., Phys. Plasmas **9** (2002) 898.
[8] ALLFREY S.J., BOTTINO A., SAUTER O., VILLARD L., New Journal of Physics **4** (2002) paper no.29, http://www.njp.org.
[9] ALLFREY S.J., et al., Proc. 29th EPS Conference on Plasma Physics and Controlled Fusion, Montreux, Switzerland, June 2002, ECA Vol.26A, (2002) P4.059 (http://epsppd.epfl.ch)
[10] ALLFREY S.J., et al., to be published in Theory of Fusion Plasmas, Proc. Joint Varenna-Lausanne International Workshop, Varenna, August 2002, edited by J.W. Connor, O. Sauter and E. Sindoni, ISPP-20 (Editrice Compositori, Bologna, 2002).
[11] KIM J.Y., HORTON W., DONG J.Q., Phys. Fluids B **5** (1993) 4030.
[12] ZONCA F., CHEN L., DONG J.Q., SANTORO R.A., Phys. Plasmas **6** (1999) 1917.
[13] JENKO F., SCOTT B.D., Phys. Rev. Lett. **80** (1998) 4883.
[14] BRUNETTI M., et al., *ibid* [9], P4.102.
[15] GRANDGIRARD V., et al., *ibid* [9], P4.095.
[16] VILLARD L., BOTTINO A., SAUTER O., VACLAVIK J., Phys. Plasmas **9** (2002) 2684.
[17] VILLARD L., et al., *ibid* [9], P4.069.
[18] BOTTINO A., et al., *ibid* [9], P1.040.
[19] BRUNNER S., FIVAZ M., TRAN T.M., VACLAVIK J., Phys. Plasmas **5** (1998) 3929.
[20] FALCHETTO G.L., et al., *ibid* [9], P5.061.
[21] DONG J.Q., CHEN L., ZONCA F., Nucl. Fusion **38** (1999) 1041.
[22] BOTTINO A., et al., *ibid* [10].
[23] JOST G., TRAN T.M., COOPER W.A., VILLARD L., APPERT K., Phys. Plasmas **8** (2001) 3321.
[24] ALLFREY S.J., BOTTINO A., HATZKY R., JOST G., VILLARD L., Proc. 28th EPS Conference on Controlled Fusion and Plasma Physics, Funchal, Madeira, Portugal, June 2001, Ed. by C. Silva, C. Varandas and D. Campbell, ECA Vol.25A, 1933 (2001) P5.042.